

This is an Open Access document downloaded from ORCA, Cardiff University's institutional repository:<https://orca.cardiff.ac.uk/id/eprint/126240/>

This is the author's version of a work that was submitted to / accepted for publication.

Citation for final published version:

Chernyshova, Maryna, Malinowski, Karol, Czarski, Tomasz, Kowalska-Strzeciwiłk, Ewa, Linczuk, Pawel, Wojenski, Andrzej, Krawczyk, Rafal Dominik and Melikhov, Yevgen 2019. Advantages of AI based GEM detector aimed at plasma soft-semi hard X-ray radiation imaging. *Fusion Engineering and Design* 146 , pp. 1039-1042. 10.1016/j.fusengdes.2019.01.153

Publishers page: <http://dx.doi.org/10.1016/j.fusengdes.2019.01.153>

Please note:

Changes made as a result of publishing processes such as copy-editing, formatting and page numbers may not be reflected in this version. For the definitive version of this publication, please refer to the published source. You are advised to consult the publisher's version if you wish to cite this paper.

This version is being made available in accordance with publisher policies. See <http://orca.cf.ac.uk/policies.html> for usage policies. Copyright and moral rights for publications made available in ORCA are retained by the copyright holders.



Advantages of Al based GEM detector aimed at plasma soft–semi hard X-ray radiation imaging

Maryna Chernyshova^a, Karol Malinowski^a, Tomasz Czarski^a, Ewa Kowalska-Strzęciwilk^a, Paweł Linczuk^{a,b}, Andrzej Wojeński^b, Rafał Dominik Krawczyk^b, Yevgen Melikhov^c

^a*Institute of Plasma Physics and Laser Microfusion, Warsaw, Poland*

^b*Warsaw University of Technology, Institute of Electronic Systems, Warsaw, Poland*

^c*School of Engineering, Cardiff University, Cardiff, United Kingdom*

Development of gaseous detectors, more specifically Gas Electron Multiplier (GEM) based detectors, for application at tokamak plasma radiation monitoring/imaging in Soft–Semi Hard X-ray (S–SH) region is an ongoing research activity aiming to deliver valuable information on plasma shape, magnetic configuration, non-axisymmetry phenomena of the plasma, etc. Wide radiation range and brightness of plasma radiation impose some restrictions on choice of materials in the detecting chamber, as their interaction with the incident radiation may disrupt original signals.

This work proposes usage of aluminum as GEM foils electrodes for the first time. The detector based on these foils was constructed and examined. The operational characteristics and spectral capabilities of such detector were compared with the ones based on the standard (commonly used) copper GEM foils. The laboratory tests were performed using X-ray tube and ⁵⁵Fe sources to examine detectors' capabilities in energy-resolved imaging. Additionally, simulations of origin and number of the generated electrons, which determine the detector signal, were performed for Al and Cu GEM foils for a wide energy range of incident photons. The experimental and modelling data demonstrated that Cu based GEM detector produces higher parasitic signal than Al one necessitating total elimination of copper from detector's chamber.

Keywords: Nuclear instruments for hot plasma diagnostics, X-ray detectors, SXR imaging, Electron multipliers (gas), Micropattern gaseous detectors, aluminum GEM foils.

1. Introduction

Among gaseous detectors utilized in high energy physics, Gas Electron Multiplier (GEM) [1] detectors play a very important role being a robust tool to study different types of radiation. Recently, they have started concurring other areas of science, e.g. plasma physics application [2-7], where GEM-based imaging technique is proposed to perform advanced imaging, capable of photon energy discrimination, which can reach a very accurate spatial and sufficient temporal resolution providing lots of information on the detected radiation: impurity distribution, slow MHD, magnetic axis, magnetic reconnection, runaway electrons study, plasma shape, etc., including data processing on the fly (in real-time) usable for plasma control purposes. Since plasma radiation is characterized by its extreme brightness and wide range, the detecting part of the diagnostics has to be adjusted to experimental conditions/environment. Not only it should examine radiation correctly, but also it should ideally not bring any parasitic additional signals originating from interaction of detector elements with the incoming radiation, e.g. fluorescence emission from the photon sensitive chamber elements. Thus, the detector elements have to be designed such that they do not disrupt an original signal making any radiation diagnostics preparation a challenge.

One of the most important elements of the detector chamber is GEM foil. It is a thin perforated Kapton film with both sides covered by a metal, with a thin chromium

layer, 7-100 nm, beneath the metal that is used for adhesion purpose. Application of high voltage (HV) differences to both sides allows amplification of the photoelectron due to creation of high electric field in the holes of the film. Historically, copper is used as a coated metal for both sides, however, this brings a problem in particular case of tokamak plasma radiation monitoring.

Tokamak plasma radiation monitoring is an effective way to study diverse plasma phenomena that is the subject of our interest. Its photon Soft–Semi Hard (S–SH) X-ray spectrum consists of wide bremsstrahlung part mixed with the heavy impurities emission. Such a spectrum, what could be crucial for ITER, extends usually above the copper absorption edge (~9 keV), the basic material used until now for the GEM foils cladding, leading to a parasitic fluorescence signal. Very preliminary studies to adapt the GEM foils were recently launched with copperless foils [8] based on chromium adhesive layer. However, Cr K_α line is at 5.411 keV, getting to the targeted photon energy range. In addition, the fluorescence yield is also high due to relatively high Z, being ~0.35 for Cr and ~0.5 for Cu [9], as well as photon absorption effect.

Aluminum is a promising candidate for GEM foil metal cladding for tokamak plasma imaging in S–SH X-ray range. The lower absorption coefficient of Al compared to Cu above 2 keV would lead to less radiative effect for Al foil and, in addition, Al fluorescence yield is less than 0.05 [9]. In this work, for the first time to the

best of authors' knowledge, a newly developed aluminum GEM foils (with Cr adhesion layer) are preliminarily tested with the aim of plasma S-SH X-ray radiation imaging exploitation.

2. Al vs. Cu GEM foils detector performances

2.1 Simulations of radiation interaction effects

In order to compare the effects of different materials on the radiation imaging, simulations of GEM detector response were performed by GEANT4 program [10], which is a platform for the simulation of particles transition through matter using Monte Carlo methods. The simulations use the Low Energy Electromagnetic Physics model taking into account, among others, such phenomena as fluorescence and Auger electron emission in atomic deexcitation. Triple-GEM detector structure was used: drift gap (5 mm) / GEM foil 1 / transfer gap (2 mm) / GEM foil 2 / transfer gap (2 mm) / GEM foil 3 / induction gap (2 mm). Each GEM foil consisted of the following layers: metal (5 μm) / Cr / Kapton (50 μm) / Cr / metal (5 μm) with metal being either Cu or Al. Two values of Cr layer thickness were chosen: 7 nm and 100 nm, to cover for typical values reported by producers of the foils. Holes were double conical with 50 μm /70 μm small/large diameters, respectively, positioned hexagonally every 140 μm . Detector's window was Mylar/Al with thicknesses of 5 μm /0.2 μm , respectively. Cu readout was used with 0.5 mm thickness. Ar/CO₂ mixture at the ratio 70/30 was used for both the simulations and experiment. Gas pressure was chosen to be 1013.25 hPa and temperature was 294.15 K. Incident X-rays were introduced randomly in vacuum just above the window and with the incident direction being (0,0,-1). The simulations were based on interaction of incident photons with energies from 0.1 keV to 1 MeV (120 monoenergetic logarithmically distributed points with the statistics of 10⁵ each) with the detector chamber and analyzing the created electrons in terms of their energy and place of origin. In general, two groups of electrons were considered in the analysis of results. One group is electrons created directly as a result of interaction of radiation striking the GEM detector (e.g. photoelectrons and Auger electrons), while the second group is electrons

formed secondarily as a result of interaction with fluorescent gammas, which also arise as a result of primary interactions.

Generally, in a GEM type detector, the mechanism of initiating the electron avalanche is such that as a result of the interaction of X-rays with the detector chamber (usually a photoelectric effect) several (~2-5) so-called δ -electrons are created. Their energy most often corresponds to the energy of the X-ray quantum. These electrons losing energy in the gas on their way cause creation of the so-called conducting, or *primary*, electrons (e.g. for 5.9 keV photon this number is ~210 electrons [11]), which are multiplied in the detector and begin the electron avalanche. In the presented spectral distributions below, the energy sum of all δ -electrons generated in a single interaction, as directly corresponding to the number of conducting (primary) electrons forming an avalanche in the GEM detector, was used.

Fig. 1 (a-b) show the total energy of δ -electrons, generated in Al GEM detecting chamber by incident photons of a given energy: (a) for all the electrons except the electrons coming from fluorescence emission of the construction materials and gas, and (b) from the fluorescence X-rays only. All considered electrons were found in the drift (conversion) region as origin of incident or secondary photon interactions, anywhere in the detector photon sensitive chamber. The results for Cu GEM based detector (not presented here) are quite similar except for the higher number of electrons generated by interaction with Cu material. Intensities of the created δ -electrons vs. the X-ray photon energy are shown for two types of GEM foils: Cu and Al in Fig. 1 (c). Several times less electrons are coming from Al GEM foils than from Cu foils: at the tail of the photoeffect (from ~10 keV) and about two times less at the middle part of Compton's effect (several hundred keV). Whereas at ~2 keV Al is expected to produce about 1.5 times more electrons.

Fig. 2 shows an example of the δ -electrons spectra for both GEM foils originated from 2.3 and 17.4 keV incident photons. Intensity of the parasitic fluorescence lines varies strongly according to the materials used in the detecting chamber. Despite slightly higher absolute intensity of Al fluorescence line as compared to Cu line,

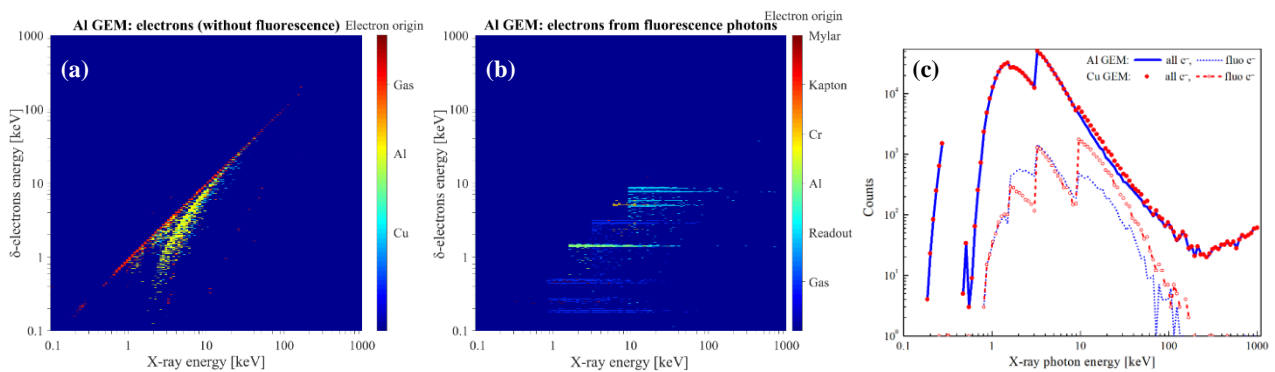


Fig. 1. δ -electrons intensity map on the incident photon energy and sum of the electrons energy for Al GEM foil based detector for: (a) all electrons except the electrons coming from fluorescence emission of the construction materials and gas, (b) electrons from the fluorescence X-rays only. (c) Intensities of δ -electrons vs. X-ray photon energy for Cu and Al GEM foils.

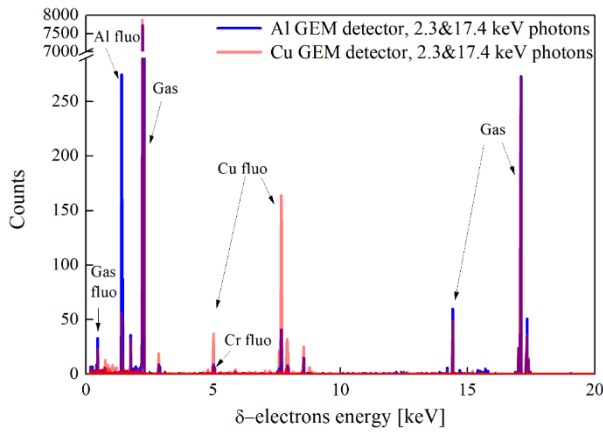


Fig. 2. Simulations of the δ -electrons spectra for 2.3 and 17.4 keV (Mo L , K -edges) incident photons for two GEM foils for 100 nm Cr layer.

the ratios of fluorescence lines to the corresponding excitation peaks must be compared to identify a better detector. Clearly, Al line intensity is only about 3% of the 2.3 keV gas line as compared to 60% of Cu line to the 17.4 keV gas line.

2.2 Experimental tests and results

The initial tests on constructed detectors showed that Al GEM based triple-GEM detector manifested less sustainability to high voltage than the Cu GEM one, i.e. more spontaneous discharges were noticed. That could be attributed to the foils' quality: microscope images in Fig. 3 showed very ragged surface of Al foils with chips on holes' edges, whilst Cu foils look very smooth over the whole surface as well as around the perforations.

In order to verify the spectral performance of both detectors the X-ray tube (Mini-X Amptek X-ray tube with Au target) was used to irradiate the targets. The following targets were used for acquiring the spectra: Al, Cu, Ti, Zn, Mo, Ag (all high purity materials), Al GEM foil and Cu GEM foil. In addition, the same targets emission was measured by the XR-100SDD Amptek detector under a condition of keeping sufficiently small dead time (less than 1% for Al, Ag, Mo, GEM foils, about 4% for Ti and 10% for Zn and Cu). All the spectra were calibrated by ^{55}Fe main line (5.9 keV) which was measured before and

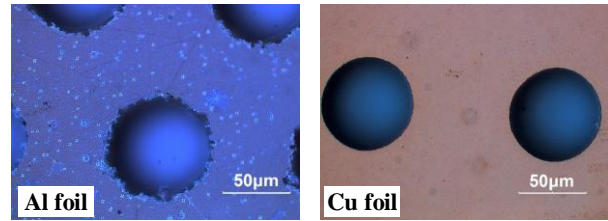


Fig. 3. Optical microscope images of Al (left) and Cu (right) GEM foils.

may result from the peak position calculation as an average value from a different environment of the maximum.

Fig. 4 shows the obtained spectra for Ag, Mo, and both GEM foils targets emission measured by both GEM and SXR SDD detectors. All the gaps were kept at the same high voltage (HV) for both detectors (1200 V for drift and 600 V for transfer/induction) differing only by the potential applied to GEM foils in order to have the same charge value produced by the target emission lines in the detector chamber. For the rest of the targets the observed spectra were identical showing just K -series emission lines. In case of Cu GEM foil detector their energies were not enough to excite the Cu elements, but in case of Al GEM foil detector Al emission was found to be at most at the noise level for all the spectra. For Al target it was found that the radiation of the K_{α} line is overlapped with the Au X-ray tube emission, which gets to the detector, so after the background subtraction the unphysical/negative count numbers were obtained. In case of Ag and Mo targets presented in Fig. 4 (a, b), the difference in the ratio of the main peaks intensities (at ~ 3 keV and 22 keV for Ag, and ~ 2.4 and 17.4 keV for Mo) is altered due to lower Ar/ CO_2 gas efficiency for higher photon energies. It also affects significantly the low photon energy peaks (1-3 keV region) modifying the peak shape/top, being drawn to the lower energy (see Fig. 2 in [11]).

The presented results (Fig. 4 (a, b)) expose also the undesired impact of Cu material. Even for Al GEM based detector with the only Cu origin from the readout board (6 mm away from the drift gap), Cu contributes to the overall signal (see the peaks at about 8 keV on both figures).

The results of irradiating GEM foil targets are presented in Fig. 4 (c). Cu GEM foil spectrum exhibits the

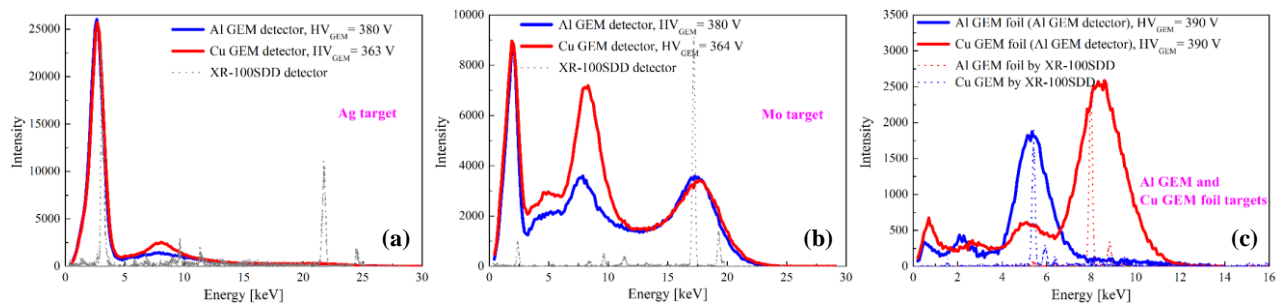


Fig. 4. Measured spectra for the following targets: (a) Ag, (b) Mo, and (c) Cu GEM and Al GEM foils.

Cu *K*-series lines (the broad peak at about 8 keV with the Ar escape peak at about 5 keV (copper line minus Ar excitation potential, 3.2 keV). The presence of chromium layer is not pronounced for this case except the small peak at about 2.5 keV, which could be the Ar escape peak related to the Cr *K*-series emission at 5.41/5.96 keV (K_α/K_β , respectively). On the contrary, for Al GEM target, the Cr line is clearly visible at ~ 5.5 keV with the Ar escape peak at ~ 2 keV. This can be explained taking into account both lower absorption and higher transmission through Al layer as compared to Cu layer.

3. Summary

Imaging plasma diagnostics with energy discrimination of plasma radiation is another promising niche for GEM based technology that is under development. However, due to extreme brightness and wide range of plasma radiation, the incoming radiation might interact with the detector's materials. Such an interaction might produce a background signal that will be added to the signal from the plasma. Limitations on the detector's materials have to be imposed therefore. It is debated that copper, commonly used metal for GEM foil, may cause problems and, therefore, aluminum was proposed as a metal for GEM foil. In this work, for the first time to the best of authors' knowledge, the response of the Al GEM foil detector was studied and compared to the common Cu GEM foil one, both theoretically and experimentally. The simulation results were found to be in agreement with the measured spectra. These results provide an important information of the detector signal origin: both material and type of interaction occurred and support the conclusion that Al is more suitable material for this application.

Differing only by the foils material, two GEM detectors were routinely tested with no difference found in the detectors' basic performance except the slightly less resilient behavior of Al GEM foil detector to the HV applied, more spontaneous discharges were observed.

As imaging imposes perpendicular direction of the incident radiation, it requires minimizing all the inexpedient input coming from the detector materials interaction with the incident rays. For this purpose, the detectors were tested under various fluorescence emission. It was found that the main contribution of the unwanted signal comes from copper present in the widely used standard GEM foils, mainly from the upper face of the first GEM foil. Both simulated and measured spectra confirmed that Al foils based detector records much lower parasitic signal. As copper is the main element of the signal readout board, its presence is also observed in Al foils based detector, although about four times smaller. This necessitates total elimination of copper material from the photon sensitive detector chamber.

Additionally, irradiating the Al GEM foil, it was found that Cr layer could contribute to the obtained spectrum if the incident photon energy is higher the Cr excitation potential. Considering its low intensity even with taken into account attenuation by Al layer, it could be sufficient

for the imaging application. The simulation performed for less thick Cr layer (7 nm vs. 100 nm used in the technological process) led to a conclusion that decreasing Cr layer could get rid of Cr effect almost totally. For even more effective elimination of the intrinsic detector lines, the Cr layer could be replaced by Ti one, which has slightly less radiative performance. This will be taken into account in the next approach of the proposed GEM detector development. In addition, one must also consider the aspect of neutron activation of the surrounding material at the fusion experiment as a source of background radiation which is a separate and broad task (see, for example, [6]).

Acknowledgments

This work has been carried out within the framework of the EUROfusion Consortium and has received funding from the European Union's Horizon 2020 research and innovation programme under grant agreement number 633053. The views and opinions expressed herein do not necessarily reflect those of the European Commission.

This work was partly supported by Polish Ministry of Science and Higher Education within the framework of the scientific financial resources in the years 2015-2018 allocated for the realization of the international co-financed project.

References

- [1] F. Sauli, The gas electron multiplier (GEM): Operating principles and applications, Nuclear Instruments and Methods in Physics Research Section A 805 (2016) 2-24.
- [2] M. Chernyshova et al., Conceptual design and development of GEM based detecting system for tomographic tungsten focused transport monitoring, Journal of Instrumentation 10 (2015) P10022.
- [3] D. Mazon et al., GEM detectors for WEST and potential application for heavy impurity transport studies, Journal of Instrumentation 11 (2016) C08006.
- [4] M. Chernyshova et al., Development of GEM detector for plasma diagnostics application: simulations addressing optimization of its performance, Journal of Instrumentation 12 (2017) C12034.
- [5] D. Mazon et al., Design of soft-X-ray tomographic system in WEST using GEM detectors, Fusion Engineering and Design 96-97 (2015) 856-860.
- [6] M. Chernyshova et al., Gaseous electron multiplier-based soft x-ray plasma diagnostics development: Preliminary tests at ASDEX Upgrade, Review of Scientific Instruments 87 (2016) 11E325.
- [7] M. Chernyshova et al., Study of the optimal configuration for a Gas Electron Multiplier aimed at plasma impurity radiation monitoring, Fusion Engineering and Design 134 (2018) 1-5.
- [8] B. Mindur et al., Performance of a GEM detector with copper-less foils, Journal of Instrumentation 12 (2017) P09020.
- [9] M. O. Krause, Atomic Radiative and Radiationless Yields

for K and L Shells, Journal of Physical and Chemical Reference Data 8 (1979) 307.

- [10] J. Allison et al., Recent developments in Geant4, Nuclear Instruments and Methods in Physics Research Section A 835 (2016) 186-225.
- [11] K. Malinowski et al., Simulation of energy spectrum of GEM detector from an x-ray quantum, Journal of Instrumentation 13 (2018) C01018.